

---

# ARQ: A Mixed-Precision Quantization Framework for Accurate and Certifiably Robust DNNs

---

Yuchen Yang<sup>1</sup> Shubham Ugare<sup>1</sup> Yifan Zhao<sup>1</sup> Gagandeep Singh<sup>1</sup> Sasa Misailovic<sup>1</sup>

## Abstract

Mixed precision quantization has become an important technique for optimizing the execution of deep neural networks (DNNs). *Certified robustness*, which provides provable guarantees about a model’s ability to withstand different adversarial perturbations, has rarely been addressed in quantization due to unacceptably high cost of certifying robustness. This paper introduces ARQ, an innovative mixed-precision quantization method that not only preserves the clean accuracy of the smoothed classifiers but also maintains their certified robustness. ARQ uses reinforcement learning to find accurate and robust DNN quantization, while efficiently leveraging randomized smoothing, a popular class of statistical DNN verification algorithms. ARQ consistently performs better than multiple state-of-the-art quantization techniques across all the benchmarks and the input perturbation levels. The performance of ARQ quantized networks reaches that of the original DNN with floating-point weights, but with only 1.5% instructions and the highest certified radius. ARQ code is available at <https://anonymous.4open.science/r/ARQ-FE4B>.

## 1. Introduction

Mixed-precision quantization has become an important technique for enabling the execution of DNNs on limited resource computing platforms. Quantization of an original DNN model with floating-point weights/activations significantly reduces the model size and the complexity of operations, while retaining the model’s accuracy. However, quantizing the model also reduces its *robustness*, i.e., the ability of the network to produce a correct classification in the presence of (even small) adversarial input perturbations.

<sup>1</sup>Department of Computer Science, University of Illinois Urbana-Champaign, Champaign, USA. Correspondence to: Yuchen Yang <yucheny8@illinois.edu>.

Preprint. Not peer-reviewed.

To alleviate this problem, *certified robustness* techniques provide formal guarantees that the DNN will classify all small perturbations with the same label as the original input. These techniques are designed to protect against a broad scope of possible adversarial inputs, unlike commonly used *empirical robustness* techniques, which defend against only a specific kind of adversarial inputs, typically in a best-effort fashion (Raghunathan et al., 2018; Li et al., 2023). Appendix A.1 presents the conceptual difference between empirical and certified robustness in more detail.

Despite their desirability, certified robustness techniques, have a high computational cost. Many deterministic techniques that have been developed have been used only on small networks and datasets (Singh et al., 2019; Lechner et al., 2022; Zhang et al., 2022). Statistical methods for robustness certification based on *randomized smoothing* (RS) (Cohen et al., 2019) currently offer the greatest scalability. Yet, due to their cost, RS and other similar techniques have not been used *during* quantization but only at the end of the optimization to characterize the level of robustness of the final quantized network. Using these techniques during model quantization has been an open question.

**Our Work: ARQ.** We present ARQ, the first mixed-precision quantization technique that can incorporate certified robustness in the optimization objective and handle state-of-the-art vision DNNs and datasets. ARQ’s algorithm takes a pre-trained DNN and encodes a reinforcement learning (RL) problem that searches for *quantization policies* – the bit-widths of the weights/activations of all layers in the DNN – that (1) preserve DNN’s accuracy, (2) improve its certified robustness, and (3) reduce the model’s computation cost and/or size. This design allows ARQ to support mixed-precision quantization (MPQ), in which the weights in each layer can be quantized with different bit-widths, thus giving fine-grained control over possible policies.

The key insight behind ARQ is that the optimization for both accuracy and robustness aims to maximize the DNN’s *certified radius*, which characterizes all the slightly perturbed inputs that the DNN classifies with the same label as the non-perturbed input. This optimization objective fits well within the RL framework and randomized smoothing is able to give probabilistic guarantees for state-of-the-art visual

inputs (e.g., ImageNet). Moreover, the design of ARQ’s algorithm makes it possible to leverage recent approaches for incremental analysis of certified robustness to further speed up the quantization policy search.

We compare ARQ with existing searching and learning-based mixed-precision quantizers that only optimize for accuracy. The baselines include RL-based HAQ (Wang et al., 2019), integer programming-based LIMPQ (Tang et al., 2023), differentiable algorithm NIPQ (Shin et al., 2023), Hessian-based HAWQ-V3 (Yao et al., 2021) and fixed-precision quantization PACT (Choi et al., 2018). We considered three DNN architectures commonly used in quantization studies: ResNet-20 on CIFAR-10, ResNet-50 on ImageNet, and MobileNetV2 on ImageNet.

We demonstrate that ARQ consistently finds DNNs with higher certified robustness and clean accuracy than these baselines across all the benchmarks and the input noise levels. In many cases, ARQ can even reach, and sometimes even improve on the accuracy and robustness of the original floating-point network, with only 1.5% operations.

**Contributions.** The paper makes several contributions:

- **Approach:** We present ARQ, the first approach for mixed-precision quantization that optimizes for certified robustness of DNNs. It poses an optimization problem that maximizes the certified radius for a bounded resource usage cost (e.g., compute instructions, model size).
- **Framework:** ARQ’s algorithm incorporates randomized smoothing within the reinforcement learning loop, which enables it to find certifiably robust quantized networks.
- **Results:** Our experiments on three commonly used networks/datasets show that ARQ finds DNNs with higher certified robustness and clean accuracy than the state-of-the-art quantization techniques.

## 2. Background

### 2.1. Mixed Precision Quantization

DNN quantization compresses the model to reduce a network’s size and compute cost. Quantization applies to float-valued weights and activations in the network and converts them to integer values of certain bit-widths. Using the same bit-width for the entire network is sub-optimal because some layers are more amenable to quantization than others.

Mixed Precision Quantization assigns different bit-widths per weight or activation in a network and searches for the best combination of bit-widths. A *quantization policy*  $P$  is a sequence of bit-width assignments to each layer in the network. For a network of  $L$  layers, where each layer has  $N$  bit-width options  $\{b_1, b_2, \dots, b_N\}$  for both weights and activations, there are  $N^{2L}$  combinations of quantization policies. We can then formulate the process of optimizing

the quantization policy  $P$  for a network  $f_P(x)$  as the following mathematical optimization problem:

$$P_{optimal} = \arg \max_{P \in \mathcal{P}} \text{Acc}(f_P(x), y) \quad \text{s.t. Cost}(f_P) < C_0 \quad (1)$$

$$\text{Acc}(f(x), y) = \frac{1}{|X|} \sum_{(x,y) \in X} \mathbf{1}(f(x) = y) \quad (2)$$

$\mathcal{P}$  is the set of all quantization policies and  $P_{optimal} \in \mathcal{P}$  is the optimal policy that maximizes the accuracy of the quantized DNN  $\text{Acc}(f_P(x))$  on dataset  $X$ .  $\text{Cost}(f_P)$  is the resource usage of the quantized DNN (e.g., the model size, the number of compute bit operations or energy consumption), and  $C_0$  is a user-specified bound on the resource. By sweeping over multiple values of  $C_0$  one can find a Pareto-optimal set of policies that maximize both accuracy and cost.

**Reinforcement Learning Based Quantization.** Wang et al. (2019); Lou et al. (2020) have introduced Reinforcement Learning (RL) based approaches to search for quantization policies. One of the popular RL algorithms is the Deep Deterministic Policy Gradient (DDPG) (Lillicrap et al., 2019) (see Appendix A.8 for details). The DDPG agent iteratively interacts with the environment (the neural network) by observing the state  $S_k$  (the configuration of the  $k_{th}$  layer), taking an action  $a_k$  (the quantization bit-width), and receiving a *Reward* (the resulting accuracy).

### 2.2. Certified Neural Network Robustness

A classifier is considered *certifiably robust* when its predictions are guaranteed to remain consistent within a neighborhood of input  $x$ . Consider a classification problem from  $\mathbb{R}^m$  to classes  $\mathcal{Y}$ . Let  $f : \mathbb{R}^m \rightarrow \mathcal{Y}$  be a neural network classifier. We seek a *smoothed* classifier  $g : \mathbb{R}^m \rightarrow \mathcal{Y}$ , whose prediction matches that from  $f$  for any input  $x$  and is *constant* within some neighborhood of  $x$ . Randomized smoothing (Cohen et al., 2019; Yang et al., 2020; Zhang et al., 2020) provides a way to construct such a smoothed classifier  $g$  from the base classifier  $f$ . When queried at  $x$ ,  $g$  returns the class that  $f$  is most likely to return when  $x$  is perturbed by Gaussian noise:

$$g(x) := \arg \max_{c \in \mathcal{Y}} \mathbb{P}(f(x + \varepsilon) = c) \quad \text{s.t. } \varepsilon \sim \mathcal{N}(0, \sigma^2 I) \quad (3)$$

Cohen et al. (2019) show that  $g$ ’s prediction is constant within an  $l_2$  ball around any input  $x$ . The radius of that ball,  $R(x)$ , is known as the *certified radius*.  $\varepsilon$  is the Gaussian noise added on the input, sampled from Gaussian distribution of mean 0 and variance  $\sigma^2 I$  ( $I$  is the identity matrix).  $\sigma$  is the noise level, a hyperparameter of the smoothed classifier  $g$  independent of the input  $x$ . The *certified accuracy* of a classifier is defined as the probability that the classifier correctly predicts the true labels of samples  $x$  for which the certified radius  $R(x)$  exceeds a certain threshold  $r$ . The *clean accuracy* is the certified accuracy when  $r = 0$ .

**Theorem 2.1** (From (Cohen et al., 2019)). Suppose  $c_A \in \mathcal{Y}$ ,  $p_A, \overline{p_B} \in [0, 1]$ . if

$$\mathbb{P}(f(x + \epsilon) = c_A) \geq \underline{p_A} \geq \overline{p_B} \geq \max_{c \neq c_A} \mathbb{P}(f(x + \epsilon) = c),$$

then  $g(x + \delta) = c_A$  for all  $\delta$  satisfying  $\|\delta\|_2 \leq \frac{\sigma}{2}(\Phi^{-1}(\underline{p_A}) - \Phi^{-1}(\overline{p_B}))$ , where  $\Phi^{-1}$  denotes the inverse of the standard Gaussian CDF.

Computing the exact probabilities  $\underline{p_A}, \overline{p_B}$  from Thm. 2.1 is intractable in general. For practical applications, RS certification utilizes sampling to estimate  $\underline{p_A}$  and  $\overline{p_B}$  using the Clopper-Pearson method (Clopper & Pearson, 1934). If using this procedure yields  $\underline{p_A} > 0.5$ , then RS algorithm sets  $\overline{p_B} = 1 - \underline{p_A}$  and computes the certified radius as

$$R(x) = \sigma \cdot \Phi^{-1}(\underline{p_A}) \quad (4)$$

via Theorem 2.1, else it returns ABSTAIN, i.e., it cannot prove the certified robustness.

### 3. ARQ Approach

#### 3.1. Problem Statement

ARQ provides a mixed precision quantization method that optimizes both the robustness and accuracy of the *quantized smoothed classifier*  $g_P$  from a base classifier  $f$ .

**Quantization Challenges.** To improve the robustness of the quantized smoothed classifier  $g_P$ , one could naively replace the accuracy metric in the formulation of an existing MPQ method (Eqn. 1) with an accuracy metric for the base classifier  $f_P$  that uses Gaussian noise-perturbed inputs. This approach does not significantly improve the robustness of the quantized smoothed classifier  $g_P$ , because:

- By taking one perturbed sample per data point, this accuracy metric is highly affected by randomness and does not capture the robustness of  $g_P$  well.
- The accuracy of base classifier  $f_P$  correlates directly with the average lower bound probability ( $\underline{p_A}$ ) as stated in Eqn. 2.1. However, improving the quantized base classifier  $f_P$ 's accuracy on samples with  $\underline{p_A} < 0.5$  does not improve the quantized smoothed classifier  $g_P$ 's accuracy. Because for samples where  $\underline{p_A} < 0.5$ , the certified radius is less than zero, indicating that the quantized smoothed classifier  $g_P$  cannot provide any robustness guarantee for these samples. Consequently, these samples cannot be correctly classified by the quantized smoothed classifier  $g_P$ , regardless of the improvements made to the base classifiers on such inputs.
- Using accuracy as the optimization goal does not accurately reflect the robustness of the neural networks. As  $R = \sigma \cdot \Phi^{-1}(\underline{p_A})$ , the radius  $R$  of  $g_P$  has a complicated relation to  $\underline{p_A}$ . Therefore, optimizing only for the accuracy of the quantized base classifier  $f_P$  may not accurately

translate to improvements in the accuracy of the quantized smoothed classifier  $g_P$ . This results in a disproportionate focus on samples with smaller certified radii, while neglecting those with larger ones, due to the non-linear relationship between  $R$  and  $\underline{p_A}$ .

**ARQ Optimization Objective.** Instead, we propose using the certified radius of smoothed classifiers to directly guide the quantization method. It is more explicit as it uses feedback from the smoothed classifiers instead of the base classifiers, and it can combine the goal of optimizing both the clean accuracy and the robustness of the smoothed classifiers. We define the following optimization problem (compare Eqn. 1) to find the optimal quantization policy:

$$\begin{aligned} P_{optimal} &= \arg \max_{P \in \mathcal{P}} (\text{Average Certified Radius}) \\ \text{s.t.} \quad \text{Cost}(f_P) &< C_0 \end{aligned} \quad (5)$$

where Average Certified Radius (ACR) is estimated as:

$$\begin{aligned} \text{ACR} &= \frac{\sigma}{|X|} \sum_{(x,y) \in X} \Phi^{-1}(\mathbb{P}(f(x + \epsilon) = y)) \\ &\quad \epsilon \sim \mathcal{N}(0, \sigma^2 I) \text{ for each input } x \end{aligned} \quad (6)$$

The  $\mathbb{P}(f_P(x + \epsilon) = y)$  here represents the lower bound of probability that base classifier  $f$  can correctly classify input  $x$  under noise  $\epsilon$ . This follows from the definition of the certified radius  $R(x) = \sigma \cdot \Phi^{-1}(\underline{p_A})$  for a given input  $x$  and  $\mathbb{P}(f(x + \epsilon) = c_A) \geq \underline{p_A}$  in Section 2.2. By averaging over inputs in the dataset  $X$ , we obtain the ACR, which provides a measure of the overall robustness of the classifier. Since the clean accuracy of smoothed classifiers is the percentage of samples with a certified radius greater than zero. By focusing on optimizing the Average Certified Radius, we can improve both the accuracy and robustness of the quantized smoothed classifiers.

Therefore, our final robustness-aware quantization problem formulation is:

$$\begin{aligned} P_{optimal} &= \arg \max_{P \in \mathcal{P}} \sum_{(x,y) \in X} \Phi^{-1}(\mathbb{P}(f_P(x + \epsilon) = y)) \\ \text{s.t.} \quad \text{Cost}(f_P) &< C_0 \end{aligned} \quad (7)$$

However, it is challenging to use this formulation to search exhaustively across quantization policies because calculating the certified radius, specifically obtaining  $\mathbb{P}(f_P(x + \epsilon) = y)$ , is expensive – this probability is estimated using the Clopper-Pearson method (Clopper & Pearson, 1934), and the confidence level is related to the number of samples, and may require thousands of samples even for a single image (Cohen et al., 2019). Instead, we employ a reinforcement learning (RL) agent to search for the optimal quantization policy  $P_{optimal}$ , which we describe next.

**Algorithm 1** ARQ Search Algorithm

**Inputs:**  $(f)$ : original DNN,  $(\sigma)$ : standard deviation,  $(X)$ : inputs to the DNN,  $(n_0)$ : number of Gaussian samples used for original certification,  $(\bar{n})$ : number of Gaussian samples used for quantized model certification,  $(n_1)$ : number of Gaussian samples used for fine-tuning quantized model,  $(C_0)$ : constraint bound on the quantized models,  $(N)$ : the number of iterations for search,  $(D)$ : empty replay buffer,  $(\mu(\cdot))$ : the policy network of the agent.

```

1: function POLICY SEARCH( $f, \sigma, X, n_0, n, n_1, C_0, N, D, \mu(\cdot)$ )
2:    $g \leftarrow$  SmoothedClassifier( $f, n_0$ );
3:    $ACR_{orig} \leftarrow$  FullRobustCertify( $g, X, \sigma$ )
4:    $P_{optimal} \leftarrow \emptyset$ ;  $Reward_{best} \leftarrow 0$ ;  $g_{P_{optimal}} \leftarrow \emptyset$ 
5:   for  $t = 1$  to  $N$  do
6:     Observe the  $k_{th}$  layer's state  $S_k$  and select action  $a_k$ 
7:      $a_k = \text{clip}(\mu(S_k) + \epsilon, a_{min}, a_{max})$ , where  $\epsilon \sim \mathcal{N}_t$ 
8:     Observe next layer's state  $S_{k+1}$ 
9:     Use done signal  $d$  to indicate if  $S_{k+1}$  is the final state
10:    Store transition  $(S_k, a_k, Reward, S_{k+1}, d)$  in  $D$ 
11:    Store  $a_k$  to list  $A$ 
12:    if  $d$  is true then
13:       $P_t \leftarrow$  CombineActionsToPolicy( $A, C_0$ )
14:       $f_P \leftarrow$  Quantize( $f, P_t$ );
15:       $f_P \leftarrow$  FineTune( $f_P, X, \sigma, n_1$ )
16:       $g_P \leftarrow$  SmoothedClassifier( $f_P, n$ )
17:       $ACR_P \leftarrow$  IncrementalRobustCertify( $g_P, X, \sigma$ )
18:       $Reward_t \leftarrow ACR_P - ACR_{orig}$ 
19:      if  $Reward_t > Reward_{best}$  then
20:         $Reward_{best} \leftarrow Reward_t$ 
21:         $P_{optimal} \leftarrow P_t$ ;  $g_{P_{optimal}} \leftarrow g_P$ 
22:      end if
23:      Set  $Reward$  for all transitions to final  $Reward_t$ 
24:      Update Q-function, policy and target network
25:    end if
26:  end for
27:  return ( $P_{optimal}, g_{P_{optimal}}$ )
28: end function

```

### 3.2. ARQ Search Algorithm

Algorithm 1 presents the ARQ algorithm, which aims to determine the optimal quantization policy for a given DNN  $f$ .

We first fully certify the robustness of  $g$ , the smoothed version of  $f$  using a large number of samples  $n_0$  with function FullRobustCertify, and store the average certified radius of  $g$  as  $ACR_{orig}$  (line 2, 3). During each iteration, our RL agent observes the  $k_{th}$  layer's configuration as state  $S_k$  and uses the policy network  $\mu(\cdot)$  learned from the previous iterations to determine an action  $a_k$  (line 7). For each layer, the agent selects two actions for the weights and the activations of that layer. The transition  $(S_k, a_k, Reward, S_{k+1}, d)$  is stored in the replay buffer  $D$  for training the agent's policy network (line 10). Here,  $Reward$  is initially left blank,  $S_{k+1}$  is the configuration of the next layer, and  $d$  is the done signal indicating if it is the last layer.

After the RL agent proposes the actions for all layers, we first transform the continuous actions in list  $A$  into discrete bit-widths and combine them into a quantization policy list  $P_t$ . Then we evaluate the resource usage of the base clas-

sifier  $f_P$ , which is quantized through  $P_t$ . If the proposed quantization policy  $P_t$  exceeds the specified resource constraint  $C_0$ , we will sequentially decrease the bit-width of each layer until the constraint is finally satisfied (line 13).

The function Quantize( $f, P_t$ ) represents the quantization on  $f$  to  $f_P$  with quantization policy  $P_t$ , where the floating-point weights and activations are mapped to integers. We finetune  $f_P$  for one epoch using  $n_1$  inputs in dataset  $X$  with Gaussian noise of size  $\sigma$  to help it recover performance (line 15). Line 16 smooth  $f_P$  into a quantized smoothed classifier  $g_P$  with  $n$  (which is  $\ll n_0$ ) samples. Function IncrementalRobustCertify certifies the robustness of  $g_P$  incrementally by reusing the information from the initial certification of  $g$  (Section 3.2.3–IRS) to obtain the ACR of  $g_P$  as  $ACR_P$ . The RL agent's reward for all actions,  $Reward_t$ , is set as  $ACR_P - ACR_{orig}$ , using the average certified radius of  $g_P$  and  $g$  to guide the learning of agent (line 18, 23). After  $N$  iterations, we obtain the optimal quantization policy  $P_{optimal}$ , with maximum average certified radius of the quantized smoothed classifier.

#### 3.2.1. QUANTIZATION POLICY SEARCH

Following previous work (He et al., 2018; Wang et al., 2019), we use DDPG as our RL agent to search the bit-widths. At the  $k_{th}$  layer of the base classifier  $f$ , the state  $S_k$  of agent is:

$$S_k = (k, c_{in}, c_{out}, s_{kernel}, s_{stride}, s_{feat}, n_{params}, i_d, i_{wa}, a_{k-1})$$

where  $c_{in}$  and  $c_{out}$  are input/output channels,  $s_{kernel}$ ,  $s_{stride}$  and  $s_{feat}$  are kernel, stride and feature map sizes,  $n_{params}$  is the parameter count,  $i_d$  and  $i_{wa}$  indicate depthwise layers and weights/activations, and  $a_{k-1}$  is the previous layer's action. The first and last layers are fixed at 8-bit quantization.

We use a continuous action space with  $a_{min} = 0$  and  $a_{max} = 1$  to keep the relative order information among different actions in line 7 of Algorithm 1. Observing the state  $S_k$  and using the policy network  $\mu(\cdot)$ , the action  $a_k$  is selected for the  $k_{th}$  layer, where  $\epsilon \sim \mathcal{N}_t$  is a noise term added for exploration in truncated normal distribution. We then round  $a_k$  into discrete bit-width  $b_k$ :

$$b_k = \text{round}((b_{min} - 0.5 + a_k \times (b_{max} - b_{min} + 1)) \quad (8)$$

with  $b_{min}$  and  $b_{max}$  here denoting the min and max bit-width.

As described in lines 10 and 13 in Algorithm 1, the actions are combined into a list  $A = (a_1, a_2, \dots, a_k, a_{k+1}, \dots, a_d)$  where  $a_d$  is the final action the agent made for the last layer. When all layers has been traversed by the agent, the list  $A$  is transformed into discrete bit-width form policy  $P_t$  for the  $t_{th}$  iteration:  $P_t = (b_1, b_2, \dots, b_k, b_{k+1}, \dots, b_d)$  which is also limited by the resource constraint  $C_0$ . When the given  $P_t$ 's resource usage exceeds  $C_0$ , the bit-width will be decreased sequentially from back to front.

### 3.2.2. ROBUSTNESS-AWARE POLICY SEARCH

Due to the high cost of certifying the robustness of the quantized smoothed classifier  $g_P$ , we perform the certification only when  $d$  is true, which indicates all actions have been taken and the entire quantization policy  $P_t$  come out. This avoids the frequent and expensive robust certification for each individual quantized layer. We define our reward function  $Reward_t$  to be related to only the average certified radius of the smoothed classifiers (line 18):

$$Reward_t = ACR_P - ACR_{orig} \quad (9)$$

where  $ACR_P$  denotes the average certified radius gained by the quantized smoothed classifier  $g_P$  through the current quantization policy  $P_t$ , and  $ACR_{orig}$  denotes the average certified radius of the original smoothed classifier  $g$ , which is a function of  $x$  as formulated in Eqn. 6.

The experiences in the form of transitions  $(S_k, a_k, Reward_t, S_{k+1}, d)$  are stored in the replay buffer  $D$  to update the Q-function, policy, and target network of the DDPG agent (line 23).

We use  $Reward_{best}$  to compare with  $Reward_t$  and find the optimal quantization policy  $P_{optimal}$ , for which the corresponding  $g_{P_{optimal}}$  achieves the highest ACR.

Since our optimization goal is to maximize the average certified radius of  $g_P$  across the entire policy  $P_t$ , we set the reward for all actions across different layers in one iteration to be the same value: the final reward  $Reward_t$ . This ensures the reward reflects the overall effectiveness of the quantization policy rather than individual layer actions, promoting a more comprehensive optimization.

### 3.2.3. IMPLEMENTATION DETAILS

**Quantization.** We use a linear quantization method, which maps the floating-point value to discrete integer values in the range  $[-c, c]$  for weights and  $[0, c]$  for activations. The quantization function  $Quantize(\cdot)$  that quantizes floating-point weight value  $v$  to  $b$ -bit integer value  $q$  can be expressed as:

$$q = \text{round}(\text{clip}(v/s, -c, c)) \times s \quad (10)$$

where  $v$  is the floating-point value, and  $q$  is the quantized value.  $s = \frac{c}{2^{b-1}-1}$  is the scaling factor.  $c$  is optimized through the KL-divergence between  $q$  and  $v$ . In the network, each layer utilizes two distinct  $c$  values for quantizing weights and activations.

**IRS for Speedup in Certification.** Due to the significant time consumption caused by both the number of iterations required for quantization policy search and the time-consuming process of certifying each iteration of the quantized neural networks, we employ Incremental Randomized Smoothing (IRS) (Ugare et al., 2024) to certify

quantized smoothed classifiers more efficiently. It is known that IRS can have similar precision to re-running RS when verifying networks that have sufficient structural similarity. Our design of ARQ algorithm aims to promote this property.

## 4. Experimental Methodology

**Networks and Datasets.** We evaluate ARQ on CIFAR-10 (Krizhevsky et al., 2009) and ImageNet (Deng et al., 2009) datasets. We conduct all experiments on CIFAR-10 and ImageNet with 4-bit equivalent quantization. We also perform ablation studies on CIFAR-10 with various quantization levels. The initial floating-point DNNs are trained with Gaussian noise of variance  $\sigma^2 \in \{0.25, 0.5, 1.0\}$  on inputs. We use ResNet-20 as the base classifier for CIFAR-10, and ResNet-50 and MobileNetV2 for ImageNet. These models are chosen because they are widely used classifiers in previous studies within the areas of quantization and robustness.

**Experimental Setup.** For the ResNets experiments, we use a 48-core Intel Xeon Silver 4214R CPU with two Nvidia RTX A5000 GPUs. For the MobileNetV2 experiments, we use an AMD EPYC 7763 CPU with four Nvidia A100 GPUs. ARQ is implemented in Python and uses PyTorch.

**Hyperparameters.** We use SGD with a momentum of 0.9 and a weight decay of  $10^{-4}$  for model training and fine-tuning following Cohen et al. (2019). During the policy search, we fine-tune the CIFAR-10 models for one epoch with a learning rate of 0.01, and the ImageNet models on a 60,000-sample subset with a learning rate of 0.001. For fine-tuning in evaluation, for CIFAR-10, we set an initial learning rate of 0.01 and scaled it by 0.1 at epoch 5. For ImageNet, we set an initial learning rate of  $10^{-3}$  and used the ReduceLROnPlateau learning rate scheduler. Fine-tuning is limited to 10 epochs, and the batch sizes are 256 for CIFAR-10 and 128 for ImageNet. A detailed description of our fine-tuning epoch choice is described in Appendix A.5. For the optimization of the DDPG agent, following Wang et al. (2019), we use ADAM (Kingma & Ba, 2017) with  $\beta_1 = 0.9$  and  $\beta_2 = 0.999$ . The learning rate is  $10^{-4}$  for the actor and  $10^{-3}$  for the critic network. During exploration, truncated normal noise with an initial standard deviation of 0.5, decaying at 0.99 per episode, is applied to the actions.

**Metrics.** We use the number of bit operations (BOPs) constraint for all methods following Yao et al. (2021). BitOPs for filter  $k$  can be represented as:  $BOPs(k) = b_w \cdot b_a \cdot |k| \cdot w_k \cdot h_k / s_k^2$  where  $b_w$  and  $b_a$  are the bitwidths for weights and activations,  $|\cdot|$  denotes the number of parameters of the filter,  $w_k, h_k, s_k$  are the spatial width, height, and stride of the filter.

**Robustness Certification.** For the evaluation, we use confidence parameters  $\alpha = 0.001$  for the certification of the original smoothed classifier  $g$ , following the setting used by

RS (Cohen et al., 2019) and IRS (Ugare et al., 2024). For policy search, we use 500 validation images,  $n_0 = 10000$ , and  $n = 500$  samples per image. For  $\zeta_x$  estimation, we use  $\alpha = 0.001$  and  $\alpha_\zeta = 0.001$  on CIFAR-10, and  $\alpha = 0.01$  and  $\alpha_\zeta = 0.01$  on ImageNet.

**Evaluation.** We compare ARQ with state-of-the-art searching and learning-based mixed-precision quantization methods HAQ (Wang et al., 2019), LIMPQ (Tang et al., 2023), NIPQ (Shin et al., 2023) and HAWQ-V3 (Yao et al., 2021) and fixed-precision quantization method PACT (Choi et al., 2018). To make the baseline methods work well, we added Gaussian noise for the inputs and used the accuracy metric on the perturbed inputs as described in Section 3.1 during the policy search process. For certifying the original smooth classifier  $g$  and quantized smooth classifier  $g^P$ , we used RS on 500 images each with  $10^6$  samples.

## 5. Experimental Results

We present our main evaluation results: (1) the robustness and clean accuracy on the datasets; (2) the runtime of ARQ’s search algorithm; and (3) selected ablation studies.

### 5.1. Robustness and Accuracy Evaluation on CIFAR-10

On CIFAR-10, we used ResNet-20 as the base classifier with  $\sigma = 0.25, 0.5, 1.0$  and various BitOPs constraints. Figure 1 presents ACR vs. BitOPs Pareto frontiers for the DNNs found by ARQ and the baseline tools.

ARQ achieved the best ACR for all experiments except on  $\sigma = 0.25$  with looser BitOPs constraint setting, where the ACR drop compared to the best baseline is under 0.001. Figure 1b presents results on  $\sigma = 0.50$ . Notably, ARQ’s 4-bit and 5-bit equivalent models outperformed the floating-point original model which was not achieved by any other methods. Figure 1c presents results on  $\sigma = 1.00$ . On 3-bit equivalent BitOPs constraint, ARQ had a 0.54% ACR drop while the best baseline had a 3.43% ACR drop. ARQ also outperformed the floating-point model with 1.5% operations.

Figure 1d shows the average clean accuracy drop achieved by the methods. ARQ’s drop is smaller (hence, clean accuracy is higher) than the other baselines. Except for the 4-bit equivalent BitOPs, ARQ outperformed all baselines. Figures in Appendix A.2 present the model size/ACR tradeoff.

### 5.2. Robustness and Accuracy Evaluation on ImageNet

Table 1 shows the results of the experiments on ImageNet. We selected a 1.5% BitOPs constraint as in CIFAR-10 experiments, it demonstrated that ARQ can achieve the accuracy and robustness of floating-point models. ARQ outperformed all other quantization methods in all settings we consider. These results show that our approach with ACR

objective is able to improve *both* the clean accuracy and robustness. For ResNet-50, ACR of the ARQ-generated network is comparable to the ACR of the original floating-point model. The clean accuracy for  $\sigma = 0.25$  and  $\sigma = 1$  is even slightly higher than the accuracy of the original network. As a result of the limited fine-tuning, for MobileNetV2, the clean accuracy and ACR are reduced compared to the floating-point model, but both are significantly higher than the alternative quantization methods. Since low  $\sigma$  certifies small radii with high accuracy but not large radii, while high  $\sigma$  certifies larger radii but with lower accuracy for smaller radii, the clean accuracy drops as  $\sigma$  increases. This observation is consistent with that in RS (Cohen et al., 2019).

Note, the other mixed-precision quantization methods could hardly outperform the ACR of fixed-precision PACT (Choi et al., 2018) on ImageNet, while ARQ significantly outperformed PACT on both networks and even the original floating-point model at  $\sigma = 1.00$  on ResNet-50.

### 5.3. Execution Time of ARQ Search and Other Methods

Table 2 presents the time consumption for different methods. We selected  $\sigma = 0.5$  as it is the median value among the tested values in the experiments. The total time includes the policy search, fine-tuning, and evaluation. The Eval time is the time for fine-tuning and evaluation of the quantized smooth classifiers. Although ARQ consumes more time than other methods, it is a one-time cost, and the previous section showed that it produces the most robust models.

### 5.4. Ablation Studies

**Reward Function Choice.** We investigate the sensitivity of the policy search to the quality of the reward function. In ARQ, ACR is used as a reward to the RL agent. An intuitive question arises: What if we use the certified accuracy of the quantized smooth classifier  $g_P$  as the reward? As noted in Section 2.2, certified accuracy is the probability that  $g_P$  correctly predicts samples  $x$  with certified radius  $R(x)$  exceeds the given threshold  $r$ . Table 3 presents the ablation study results on 3-bit equivalent quantized ResNet-20 models. "Val" and "Acc" denote using the validation accuracy of  $f_P$  and the clean accuracy of  $g_P$ . "ACR+Acc" combines ACR with the accuracy of  $g_P$  as the reward function.  $\text{Acc}_{0.5}$  represents the certified accuracy of  $g_P$  at  $r = 0.5$ . We observe that "Acc" achieves better-certified accuracy at targeted  $r$  but underperforms at other radii and in ACR.

**The Effect of Incremental RS.** In our experiments, IRS is beneficial, running 1.32x faster than RS, consistent with the results from (Ugare et al., 2024). Table 5 in Appendix A.3 shows the detailed results of using RS instead of IRS to obtain  $ACR_p$  and  $Reward_t$ . Moreover, using IRS does not reduce the quality of the quantization policy (and in many cases improves it), as ARQ’s algorithm design makes

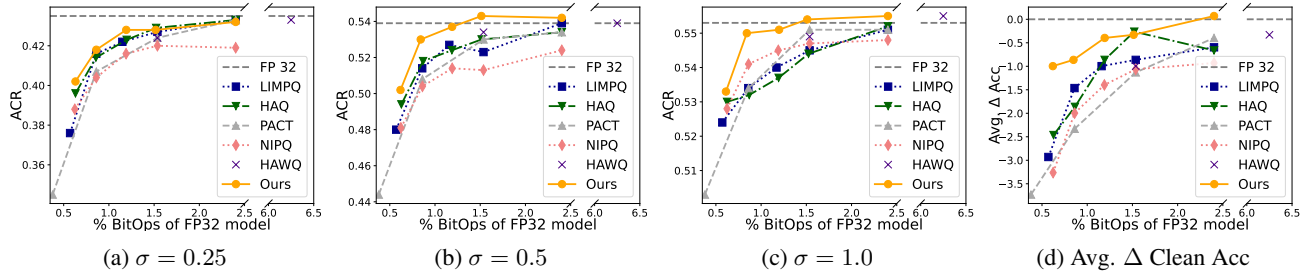


Figure 1: Experiments on CIFAR-10. The x-axis shows the percentage of BitOps of  $f_P$  relative to the original floating-point  $f$ . The y-axis shows the ACR for the first three subfigures, and the average difference in clean accuracy between the methods and the original floating-point network across different  $\sigma$  settings for Figure 1d.

Table 1: Experiments on ImageNet. The ACR denotes the average certified radius, Acc denotes the clean accuracy of the smoothed classifiers, BOPs denotes the number of bit operations of the models (in G), and Size is the model size (in MB).

Method	$\sigma = 0.25$				$\sigma = 0.50$				$\sigma = 1.00$				
	ACR	Acc	BOPs	Size	ACR	Acc	BOPs	Size	ACR	Acc	BOPs	Size	
ResNet-50	FP 32	0.488	69.4	4244.3	97.29	0.743	62.4	4244.3	97.29	0.914	45.4	4244.3	97.29
	<b>ARQ</b>	<b>0.472</b>	<b>70.8</b>	<b>63.32</b>	13.99	<b>0.724</b>	<b>61.2</b>	<b>63.50</b>	<b>13.06</b>	<b>0.916</b>	<b>46.0</b>	<b>63.50</b>	12.70
	LIMPQ	0.458	68.6	63.55	<b>13.08</b>	0.700	58.2	63.55	13.46	0.871	44.4	63.55	13.25
	NIPQ	0.460	68.4	63.56	13.21	0.696	58.8	63.56	13.07	0.885	45.0	63.56	12.96
	HAQ	0.460	69.0	63.56	13.14	0.715	60.8	64.15	13.35	0.880	44.8	63.55	<b>11.93</b>
	HAWQ	0.464	69.2	63.56	13.14	0.716	60.8	63.56	13.14	0.891	44.8	63.56	13.14
	PACT	0.460	69.0	63.56	13.14	0.715	61.0	63.56	13.14	0.884	45.4	63.56	13.14
MobileNet-V2	FP 32	0.457	67.0	308.24	13.24	0.668	57.0	308.24	13.24	0.846	44.4	308.24	13.24
	<b>ARQ</b>	<b>0.385</b>	<b>62.0</b>	<b>4.60</b>	2.23	<b>0.576</b>	<b>54.0</b>	<b>4.60</b>	<b>2.13</b>	<b>0.774</b>	<b>41.6</b>	<b>4.60</b>	2.27
	LIMPQ	0.347	58.4	4.62	2.16	0.540	50.6	4.62	2.24	0.703	40.2	4.62	2.16
	NIPQ	0.335	56.2	4.62	<b>2.09</b>	0.542	50.2	4.62	2.29	0.694	39.2	4.62	<b>2.11</b>
	HAQ	0.341	56.0	4.60	2.27	0.573	53.4	4.60	2.24	0.683	39.8	4.61	2.17
	HAWQ	0.358	58.0	4.62	2.27	0.554	51.6	4.62	2.27	0.712	40.0	4.62	2.27
	PACT	0.376	60.2	4.62	2.27	0.564	52.4	4.62	2.27	0.757	40.2	4.62	2.27

Table 2: The total time for ARQ and other quantization search approaches (in hours).

Benchmark	Policy Search				Eval
	ARQ	HAQ	LIMPQ	NIPQ	
ResNet-50	71.89	42.65	23.74	121.39	32.86
MobileNetV2	67.83	29.37	14.35	78.31	17.61
ResNet-20	2.83	2.31	0.09	0.717	0.47

subsequent candidate quantized networks similar enough to benefit from incremental robustness proving.

**Other Ablation Studies.** ARQ effectively learns mixed-precision quantization policies with different  $\sigma$  values leading to distinct policies (Appendix A.4). Extending fine-tuning from 10 to 90 epochs maintains the observed trends in ACR and accuracy (Appendix A.5). While reducing policy search time slightly impacts performance, ARQ still surpasses baselines with less time (Appendix A.6).

## 6. Related Work

**Mixed-Precision Quantization.** To optimize the balance between the accuracy and efficiency of DNNs, many mixed-precision quantization methods have been presented. Dong et al. (2019); Louizos et al. (2017); Chen et al. (2021); Tang et al. (2023) employed appropriate proxy metrics that indicate model sensitivity to quantization to generate quantization policies. Some other researchers formulated quantization policy optimization as a search problem and addressed it using a Markov Decision Process through reinforcement learning (Wang et al., 2019; Lou et al., 2020; Elthakeb et al., 2020) and a differentiable search process employed Neural Architecture Search algorithms (Guo et al., 2020; Wu et al., 2018). As Table 1 shows, ARQ outperformed HAQ (Wang et al., 2019) and LIMPQ (Tang et al., 2023), which are state-of-the-art mixed-precision quantization methods.

**Robustness of Quantized Models.** Empirical robustness approaches can improve best-effort robustness only to cer-

Table 3: Impact of the reward function on ResNet-20 for CIFAR-10 with  $\sigma = 0.5$ . The method here refers to the different approaches for the reward function.

Method	BOPs	ACR	Radius r							
			0.0	0.25	0.50	0.75	1.00	1.25	1.50	1.75
FP 32	42.04	0.539	68.2	56.0	44.6	33.8	21.8	14.4	7.2	3.8
<b>ARQ</b>	<b>0.354</b>	<b>0.530</b>	<b>67.2</b>	54.6	43.2	32.6	<b>22.2</b>	<b>14.2</b>	<b>7.4</b>	<b>4.4</b>
Val	0.363	0.518	66.4	53.4	43.0	<b>32.8</b>	21.6	13.0	<b>7.4</b>	4.0
Acc	0.360	0.512	67.0	53.2	42.6	31.4	20.4	13.2	6.8	3.6
Acc <sub>0.5</sub>	0.362	0.525	65.8	<b>55.6</b>	<b>43.8</b>	31.8	21.6	13.0	<b>7.4</b>	4.0
ACR+Acc	0.362	0.526	<b>67.2</b>	54.2	<b>43.8</b>	31.6	21.2	13.6	7.2	4.2

Table 4: Comparison of various robustness-aware model reduction methods. **Model Reduction Method:** P – Pruning; SPQ – Single-Precision Quantization; MPQ – Mixed-Precision Quantization. **Stage:** T – Training; PT – Post-training (tuning). **Scale:** Largest supported data-set.

Approach	Properties					
	Randomized Smoothing	Determ. Certify	Empirical robustness	Approx. Method	Stage	Scale
ARQ	✓			MPQ	PT	ImageNet
ATMC			✓	SPQ	T	CIFAR-100
DQ			✓	SPQ	T	CIFAR-10
GRQR			✓	SPQ	PT	ImageNet
ICR	✓			SPQ	T	Caltech-101
QIBP		✓		SPQ	T	CIFAR-10
ARMC			✓	P	T	CIFAR-10
QUANOS			✓	MPQ	PT	CIFAR-100
S-Shield			✓	SPQ	PT	CIFAR-10
HYDRA	✓*	✓*	✓	P	PT	CIFAR-10
TCR			✓	P	PT	CIFAR-10
DNR			✓	P	T	Tiny-ImageNet
HMBDT		✓		SPQ	PT	MNIST
TCMR		✓		SPQ	PT	CIFAR-10

tain adversarial inputs, but they lack the formal guarantees offered by certified methods (Raghunathan et al., 2018; Li et al., 2023). In contrast, certified robustness provides provable protection within a specified perturbation radius and thus delivers stronger safety guarantees. These two categories of approaches are inherently different in their scope and cannot be directly compared in terms of overall safety. Details on how empirical and certified robustness diverge are provided in Appendix A.1.

Several methods address the complementary challenge of training DNNs on safety-critical and resource-limited applications. ATMC (Gui et al., 2019) unified various existing compression techniques. DQ (Lin et al., 2019) and GRQR (Alizadeh et al., 2020) presented how controlling the magnitude of adversarial gradients can be used to construct a defensive quantization method.

As illustrated in Table 4, ARQ stands out by being the only approach that combines mixed-precision quantization with

post-training optimization to achieve certified robustness on large-scale datasets like ImageNet. This distinguishes our work from other approaches that either focus only on pruning (which removes over 90% of the weights) and often target smaller datasets. Although ICR (Lin et al., 2021) proposed quantization methods with RS during training, ARQ focuses on post-training optimization and has demonstrated scalability to ImageNet (compared to ICR’s much smaller Caltech-101). Appendix A.7 provides a detailed comparison between ICR and ARQ. HYDRA (Sehwag et al., 2020) analyzes pruning methods with RS but only scales to CIFAR-10 for RS and is hard to transfer to quantization methods.

## 7. Conclusion and Limitations

**Conclusion.** We introduce ARQ, the first mixed-precision quantization framework that optimizes both DNN’s accuracy and certified robustness by limiting the computational budget. By using direct feedback from the ACR of the quantized smoothed classifier, ARQ more effectively searches for the optimal quantization policy. Our experiments demonstrate that ARQ consistently outperforms state-of-the-art quantization methods, often reaching or improving the accuracy and robustness of the original FP32 networks with down to 0.84% operations. ARQ significantly reduces the computational requirements of randomized smoothing, making it possible to deploy in resource-constrained environments while providing certifiable robustness guarantees.

**Limitations.** We showed that ARQ can achieve well-quantized DNNs that match or even surpass the accuracy and robustness of the original floating-point DNNs. However, these properties are still dependent on the training of the original network, which should be trained with Gaussian augmentation. Deploying DNNs with mixed-precision quantization can be more challenging compared to the fixed-precision, however, recent works aim to address this issue (Sharma et al., 2018). The ARQ implementation has been evaluated solely on image classification tasks. Future work will explore its applicability to other complex tasks, such as object detection and natural language processing.

## Impact Statement

This paper presents work whose goal is to advance the field of Machine Learning. There are many potential societal consequences of our work, none which we feel must be specifically highlighted here.

## References

- Achiam, J. Spinning up in deep rl, 2018. URL <https://spinningup.openai.com/en/latest/algorithms/ddpg.html#the-policy-learning-side-of-ddpg>.
- Alizadeh, M., Behboodi, A., van Baalen, M., Louizos, C., Blankevoort, T., and Welling, M. Gradient  $\ell_1$  regularization for quantization robustness, 2020. URL <https://arxiv.org/abs/2002.07520>.
- Athalye, A. and Carlini, N. On the robustness of the cvpr 2018 white-box adversarial example defenses, 2018. URL <https://arxiv.org/abs/1804.03286>.
- Carlini, N. and Wagner, D. Defensive distillation is not robust to adversarial examples, 2016. URL <https://arxiv.org/abs/1607.04311>.
- Chen, W., Wang, P., and Cheng, J. Towards mixed-precision quantization of neural networks via constrained optimization, 2021.
- Choi, J., Wang, Z., Venkataramani, S., Chuang, P. I.-J., Sriniwasan, V., and Gopalakrishnan, K. Pact: Parameterized clipping activation for quantized neural networks, 2018.
- Clopper, C. J. and Pearson, E. S. The use of confidence or fiducial limits illustrated in the case of the binomial. *Biometrika*, 26(4):404–413, 1934. ISSN 00063444. URL <http://www.jstor.org/stable/2331986>.
- Cohen, J. M., Rosenfeld, E., and Kolter, J. Z. Certified adversarial robustness via randomized smoothing. In Chaudhuri, K. and Salakhutdinov, R. (eds.), *Proceedings of the 36th International Conference on Machine Learning, ICML 2019, 9-15 June 2019, Long Beach, California, USA*, volume 97 of *Proceedings of Machine Learning Research*, pp. 1310–1320. PMLR, 2019. URL <http://proceedings.mlr.press/v97/cohen19c.html>.
- Deng, J., Dong, W., Socher, R., Li, L.-J., Li, K., and Fei-Fei, L. Imagenet: A large-scale hierarchical image database. In *2009 IEEE conference on computer vision and pattern recognition*, pp. 248–255. Ieee, 2009.
- Dong, Z., Yao, Z., Gholami, A., Mahoney, M., and Keutzer, K. Hawq: Hessian aware quantization of neural networks with mixed-precision, 2019.
- Elthakeb, A. T., Pilligundla, P., Miresghallah, F., Yazdanbakhsh, A., and Esmaeilzadeh, H. Releq: A reinforcement learning approach for deep quantization of neural networks, 2020.
- Goodfellow, I. J., Shlens, J., and Szegedy, C. Explaining and harnessing adversarial examples, 2015. URL <https://arxiv.org/abs/1412.6572>.
- Gui, S., Wang, H., Yu, C., Yang, H., Wang, Z., and Liu, J. Model compression with adversarial robustness: A unified optimization framework, 2019.
- Guo, Z., Zhang, X., Mu, H., Heng, W., Liu, Z., Wei, Y., and Sun, J. Single path one-shot neural architecture search with uniform sampling, 2020.
- He, Y., Lin, J., Liu, Z., Wang, H., Li, L.-J., and Han, S. *AMC: AutoML for Model Compression and Acceleration on Mobile Devices*, pp. 815–832. Springer International Publishing, 2018. ISBN 9783030012342. doi: 10.1007/978-3-030-01234-2\_48. URL [http://dx.doi.org/10.1007/978-3-030-01234-2\\_48](http://dx.doi.org/10.1007/978-3-030-01234-2_48).
- Kingma, D. P. and Ba, J. Adam: A method for stochastic optimization, 2017.
- Krizhevsky, A., Nair, V., and Hinton, G. Cifar-10 (canadian institute for advanced research). 2009. URL <http://www.cs.toronto.edu/~kriz/cifar.html>.
- Lechner, M., Đorđe Žikelić, Chatterjee, K., Henzinger, T. A., and Rus, D. Quantization-aware interval bound propagation for training certifiably robust quantized neural networks, 2022. URL <https://arxiv.org/abs/2211.16187>.
- Li, L., Xie, T., and Li, B. Sok: Certified robustness for deep neural networks. In *2023 IEEE symposium on security and privacy (SP)*, pp. 1289–1310. IEEE, 2023.
- Lillicrap, T. P., Hunt, J. J., Pritzel, A., Heess, N., Erez, T., Tassa, Y., Silver, D., and Wierstra, D. Continuous control with deep reinforcement learning, 2019. URL <https://arxiv.org/abs/1509.02971>.
- Lin, H., Lou, J., Xiong, L., and Shahabi, C. Integer-arithmetic-only certified robustness for quantized neural networks, 2021. URL <https://arxiv.org/abs/2108.09413>.
- Lin, J., Gan, C., and Han, S. Defensive quantization: When efficiency meets robustness, 2019.
- Lou, Q., Guo, F., Liu, L., Kim, M., and Jiang, L. Autoq: Automated kernel-wise neural network quantization, 2020.
- Louizos, C., Ullrich, K., and Welling, M. Bayesian compression for deep learning, 2017.

- Madry, A., Makelov, A., Schmidt, L., Tsipras, D., and Vladu, A. Towards deep learning models resistant to adversarial attacks, 2019. URL <https://arxiv.org/abs/1706.06083>.
- Prakash, A., Moran, N., Garber, S., DiLillo, A., and Storer, J. Deflecting adversarial attacks with pixel deflection, 2018. URL <https://arxiv.org/abs/1801.08926>.
- Raghunathan, A., Steinhardt, J., and Liang, P. Certified defenses against adversarial examples. *arXiv preprint arXiv:1801.09344*, 2018.
- Sehwag, V., Wang, S., Mittal, P., and Jana, S. Hydra: Pruning adversarially robust neural networks, 2020. URL <https://arxiv.org/abs/2002.10509>.
- Sharma, H., Park, J., Suda, N., Lai, L., Chau, B., Kim, J. K., Chandra, V., and Esmaeilzadeh, H. Bit fusion: Bit-level dynamically composable architecture for accelerating deep neural network. In *2018 ACM/IEEE 45th Annual International Symposium on Computer Architecture (ISCA)*, pp. 764–775, 2018. doi: 10.1109/ISCA.2018.00069.
- Shin, J., So, J., Park, S., Kang, S., Yoo, S., and Park, E. Nipq: Noise proxy-based integrated pseudo-quantization, 2023. URL <https://arxiv.org/abs/2206.00820>.
- Singh, G., Gehr, T., Püschel, M., and Vechev, M. Boosting robustness certification of neural networks. In *International Conference on Learning Representations*, 2019.
- Tang, C., Ouyang, K., Wang, Z., Zhu, Y., Wang, Y., Ji, W., and Zhu, W. Mixed-precision neural network quantization via learned layer-wise importance, 2023.
- Tramèr, F., Kurakin, A., Papernot, N., Goodfellow, I., Boneh, D., and McDaniel, P. Ensemble adversarial training: Attacks and defenses, 2020. URL <https://arxiv.org/abs/1705.07204>.
- Ugare, S., Suresh, T., Banerjee, D., Singh, G., and Misailovic, S. Incremental randomized smoothing certification. In *The Twelfth International Conference on Learning Representations*, 2024. URL <https://openreview.net/forum?id=SdeAPVlirk>.
- Wang, K., Liu, Z., Lin, Y., Lin, J., and Han, S. Haq: Hardware-aware automated quantization with mixed precision, 2019.
- Wu, B., Wang, Y., Zhang, P., Tian, Y., Vajda, P., and Keutzer, K. Mixed precision quantization of convnets via differentiable neural architecture search, 2018.
- Yang, G., Duan, T., Hu, J. E., Salman, H., Razenshteyn, I., and Li, J. Randomized smoothing of all shapes and sizes, 2020.
- Yao, Z., Dong, Z., Zheng, Z., Gholami, A., Yu, J., Tan, E., Wang, L., Huang, Q., Wang, Y., Mahoney, M. W., and Keutzer, K. Hawqv3: Dyadic neural network quantization, 2021. URL <https://arxiv.org/abs/2011.10680>.
- Zhang, D., Ye, M., Gong, C., Zhu, Z., and Liu, Q. Black-box certification with randomized smoothing: A functional optimization based framework. In Larochele, H., Ranzato, M., Hadsell, R., Balcan, M., and Lin, H. (eds.), *Advances in Neural Information Processing Systems*, volume 33, pp. 2316–2326. Curran Associates, Inc., 2020. URL [https://proceedings.neurips.cc/paper\\_files/paper/2020/file/1896a3bf730516dd643ba67b4c447d36-Paper.pdf](https://proceedings.neurips.cc/paper_files/paper/2020/file/1896a3bf730516dd643ba67b4c447d36-Paper.pdf).
- Zhang, H., Wang, S., Xu, K., Wang, Y., Jana, S., Hsieh, C.-J., and Kolter, Z. A branch and bound framework for stronger adversarial attacks of ReLU networks. In *Proceedings of the 39th International Conference on Machine Learning*, volume 162, pp. 26591–26604, 2022.

## A. Appendix

### A.1. The differences between Certified robustness and Empirical robustness

Figure 2 compares empirical robustness and certified robustness. Empirical robustness methods rely on known adversarial attack methods during both training and testing. Although it is effective against specific attack strategies, they do not provide guarantees against future or unseen adversarial methods. Certified robustness methods ensure that the model’s predictions remain unchanged within a mathematically guaranteed region around the input. By certifying robustness during both training and testing, these methods offer provable guarantees against all bounded perturbations, including those from unknown adversarial methods.

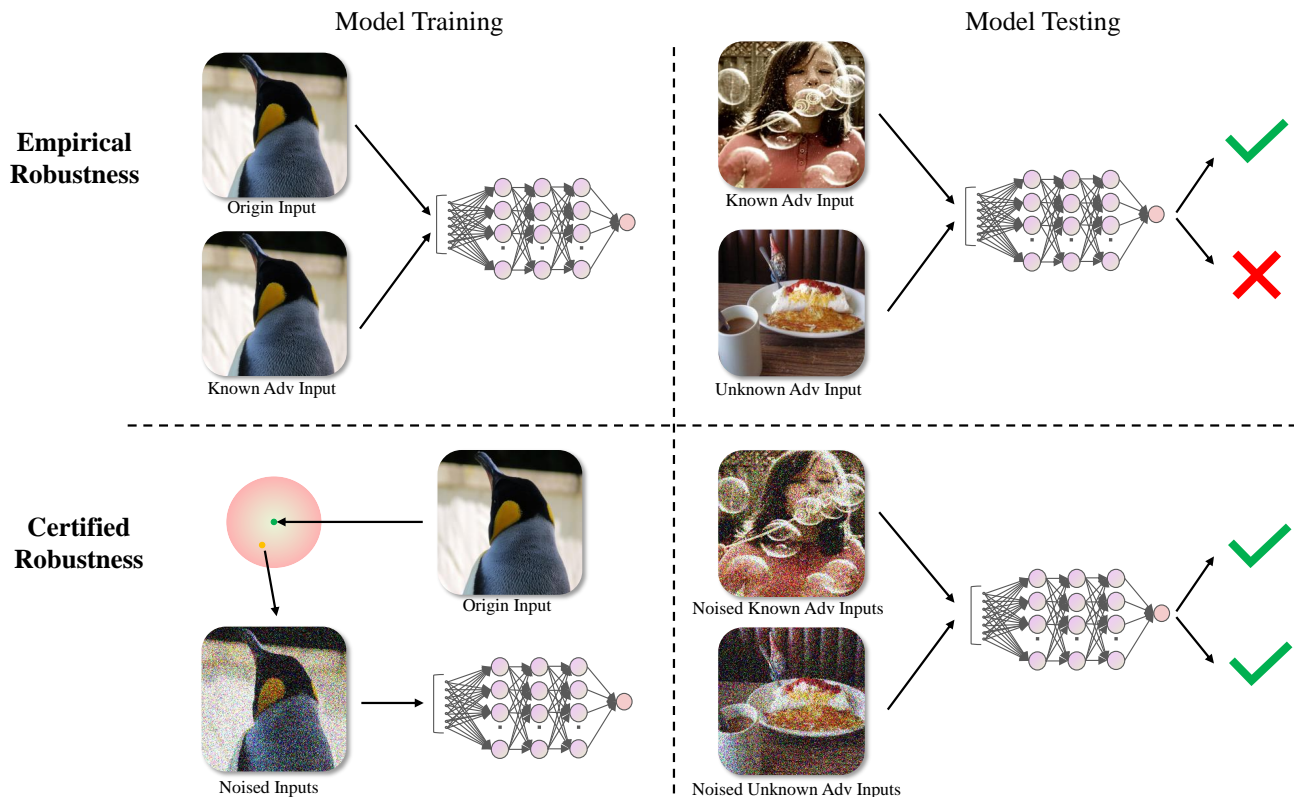


Figure 2: The figure illustrates the difference between empirical robustness and certified robustness. Images are from ImageNet and fed into ResNet-50. The noisy image has a noise level of 0.25. Known adversarial examples use FGSM (Goodfellow et al., 2015), and unknown attacks use PGD (Madry et al., 2019). The empirical defense method is Pixel Deflection (Prakash et al., 2018).

### A.2. Model Size Analysis in CIFAR-10 Experiments

In our CIFAR-10 experiments, we used ResNet-20 as the base classifier with  $\sigma = \{0.25, 0.5, 1.0\}$  and various BitOPs constraint settings. While our primary experiments focused on using BitOPs as the constraint, here we present supplementary results with ACR and average difference in clean accuracy as the y-axis and model size as the x-axis. This analysis provides additional insights into model size measurements, even though model size was not used as a constraint in our main experiments. Figure 3 compares ARQ with baseline methods.

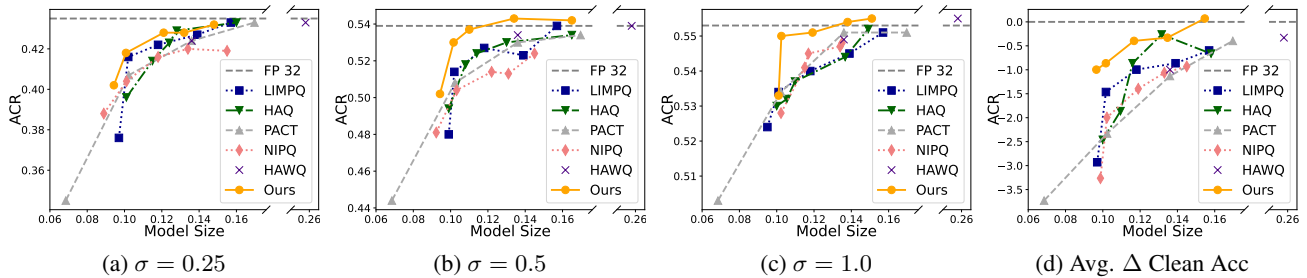


Figure 3: Experiments on CIFAR-10. The x-axis shows the model size of  $f_P$ . The y-axis shows the ACR for the first three subfigures, and the average difference in clean accuracy between the methods and the original FP32 network across different  $\sigma$  settings for Figure 1d.

A.3. Ablation Study: The Effect of Incremental RS

Table 5: The effect of incremental RS (IRS) vs rerunning RS on CIFAR-10.

Method	$\sigma = 0.25$			$\sigma = 0.50$			$\sigma = 1.00$		
	ACR	Acc	BOPs	ACR	Acc	BOPs	ACR	Acc	BOPs
FP 32	0.435	76.4	42.04	0.539	68.2	42.04	0.553	50.8	42.04
<b>ARQ(-IRS)</b>	<b>0.418</b>	<b>76.0</b>	<b>0.362</b>	<b>0.530</b>	<b>67.2</b>	<b>0.354</b>	<b>0.550</b>	<b>49.6</b>	<b>0.354</b>
ARQ-RS	0.414	75.8	<b>0.362</b>	0.526	<b>67.2</b>	0.359	0.537	49.2	0.359

A.4. Ablation Study: The quantization policies for different layers

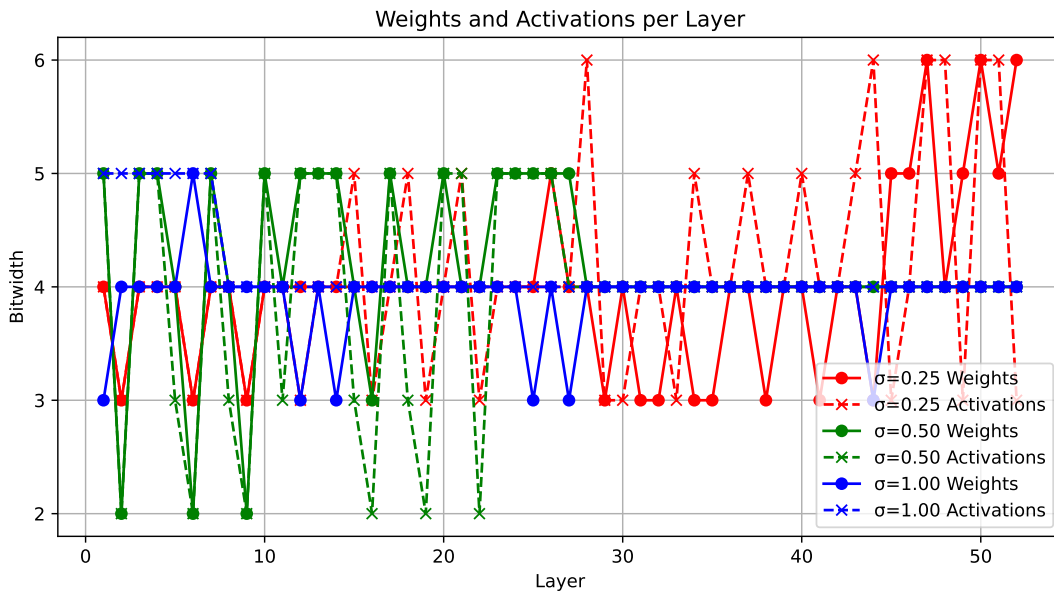


Figure 4: Quantization policy among different  $\sigma$ s for ResNet-50 on ImageNet. The x-axis represents the layer index, and the y-axis represents the bit-width selection in the quantization policy for each specific layer. The  $\bullet$  symbol represents the bit-widths for weights, and the  $\times$  symbol represents the bit-widths for activations.

Figure 4 illustrates the significance of generating different quantization policies for different values of  $\sigma$ . The quantization policy for  $\sigma = 0.25$  is more aggressive in the first half of the layers and more conservative in the later layers. This pattern is different from that of  $\sigma = 0.5$  and  $\sigma = 1.0$ , where the policy tends to make more adjustments in the first half and remains stable in the latter half.

### A.5. Ablation Study: The effect of the number of epochs in fine-tuning

Due to the limitation of computational resources, we only conducted fine-tuning for 10 epochs in our experiments. Table 6 shows the results of further fine-tuning for a total of 90 epochs. The trends in ACR and clean accuracy followed the same pattern as observed during the initial 10 epochs, demonstrating the effectiveness of our work.

Table 6: Experiments for ResNet-20 on CIFAR-10. The Epochs here indicates the number of epochs used for fine-tuning. The rest of Formats are similar to Table 1

Method	GBitOPs	Epochs = 90		Epochs = 10	
		ACR	Acc	ACR	Acc
<b>ARQ</b>	<b>0.354</b>	<b>0.545</b>	<b>67.6</b>	<b>0.530</b>	<b>67.2</b>
LIMPQ	0.361	0.535	67.0	0.514	65.0
HAQ	0.365	0.534	66.8	0.518	66.4
PACT	0.362	0.524	66.6	0.508	65.8

### A.6. Ablation Study: Further analysis on the effect of time consumption in policy search

Table 7: Performance of ARQ across different policy search time, showing corresponding clean accuracy, ACR, and BOPs.

Time	Accuracy	ACR	BOPs
3.30	67.2	0.530	0.354
2.65	66.8	0.528	0.354
0.72	66.2	0.521	0.354

Table 7 presents the results of ARQ under different time constraints for policy search. This information serves as a reference for users aiming to balance time consumption in policy optimization with accuracy and robustness during inference. Notably, although performance declines with reduced search time, ARQ still outperforms the baselines.

### A.7. Comparison experiments with robust-aware quantization methods

Table 8: Comparison experiment with RS-based quantization method ICR on ResNet-20 for CIFAR-10 with  $\sigma = 0.5$ .

Method	BOPs	$\Delta$ Acc on Radius r						
		0.0	0.25	0.50	0.75	1.00	1.25	1.50
<b>ARQ</b>	<b>0.354</b>	<b>-1.0</b>	<b>-1.4</b>	<b>-1.4</b>	<b>-1.2</b>	<b>0.4</b>	<b>-0.2</b>	<b>0.2</b>
ICR	2.596	-2.0	-2.0	-4.0	-3.0	0	<b>0</b>	-1.0

Table 8 compares the accuracy loss of ARQ and ICR (Lin et al., 2021) relative to FP32 models. Our experiments show that the 3-bit equivalent model of ARQ outperforms ICR’s 8-bit equivalent model in both clean and robust accuracy.

While empirical robustness methods are effective against known attacks, it has been shown that stronger adversaries often render them ineffective (Tramèr et al., 2020; Athalye & Carlini, 2018; Carlini & Wagner, 2016). This shows the limitations of empirical robustness that it lacks formal guarantees and remains vulnerable to new attacks. In contrast, certified robustness provides the guarantees against all perturbations within a given norm. This ensures worst-case robustness rather than best-effort defenses. And certified robustness covers a wider range of adversarial attacks, including those not explicitly tested

in empirical evaluations. As stated above, we did not compare ARQ with existing empirical robust-aware quantization methods.

### A.8. The Deep Deterministic Policy Gradient (DDPG) algorithm

DDPG learns a Q-function and a policy concurrently. It uses off-policy data and the Bellman equation to learn the Q-function, and then uses the Q-function to learn the policy.

Algorithm 2 (Achiam, 2018) shows the DDPG algorithm. In some RL search-based mixed-precision quantization methods, DDPG is utilized to search for the optimal quantization policy. The environment is usually set to be the DNN itself, state  $s$  is usually set to be the configuration of one layer in the DNN, the action  $a$  is the continuous value that can be transformed into the bit-width for the layer, and  $r$  is the reward set to be the accuracy of the DNN and computed only after all actions have been taken. The reward for all actions in one episode is set to be the final accuracy gained. The agent updates only when all actions have been taken and the reward is obtained. The experiences are stored in replay buffer  $D$  and randomly sampled in batch  $B$  for updating the Q-function, policy network, and the target network of the agent.

---

#### Algorithm 2 Deep Deterministic Policy Gradient

---

**Inputs:** Initial policy parameters  $\theta$ , Q-function parameters  $\phi$ , empty replay buffer  $D$

- 1: Set target parameters equal to main parameters:  $\theta_{\text{targ}} \leftarrow \theta, \phi_{\text{targ}} \leftarrow \phi$
- 2: **repeat**
- 3:   Observe state  $s$  and select action  $a = \text{clip}(\mu_{\theta}(s) + \epsilon, a_{\text{low}}, a_{\text{high}})$ , where  $\epsilon \sim \mathcal{N}(0, \sigma^2)$
- 4:   Execute  $a$  in the environment
- 5:   Observe next state  $s'$ , reward  $r$ , and done signal  $d$  to indicate whether  $s'$  is terminal
- 6:   Store transition  $(s, a, r, s', d)$  in replay buffer  $D$
- 7:   Set the environment state to  $s'$ . If  $d$  is true, reset the environment state
- 8:   The reward for all layers is set to be the final reward
- 9:   **if** it's time to update **then**
- 10:     **for** each update step **do**
- 11:       Randomly sample a batch of transitions  $B = \{(s_i, a_i, r_i, s'_i, d_i)\}$  from  $D$
- 12:       Compute targets for each transition:

$$y_i = r_i + (1 - d_i) \gamma Q_{\phi_{\text{targ}}}(s'_i, \mu_{\theta_{\text{targ}}}(s'_i))$$

- 13:       Update Q-function by one step of gradient descent using:

$$\phi \leftarrow \phi - \lambda_Q \nabla_{\phi} \left( \frac{1}{|B|} \sum_{i \in B} (Q_{\phi}(s_i, a_i) - y_i)^2 \right)$$

- 14:       Update policy by one step of gradient ascent using:

$$\theta \leftarrow \theta + \lambda_{\mu} \frac{1}{|B|} \sum_{i \in B} \nabla_{\theta} \mu_{\theta}(s_i) \nabla_a Q_{\phi}(s_i, a) \Big|_{a=\mu_{\theta}(s_i)}$$

- 15:       Update target networks with:

$$\theta_{\text{targ}} \leftarrow \tau \theta + (1 - \tau) \theta_{\text{targ}}$$

$$\phi_{\text{targ}} \leftarrow \tau \phi + (1 - \tau) \phi_{\text{targ}}$$

- 16:     **end for**
  - 17:   **end if**
  - 18: **until** convergence
-